33rd Annual International Conference of the IEEE EMBS
Boston, Massachusetts USA, August 30 - September 3, 2011

Influence of White Matter Conductivity Anisotropy on Electric Field Strength Induced by Electroconvulsive Therapy

Won Hee Lee, *Student Member, IEEE*, Zhi-De Deng, *Student Member, IEEE*, Andrew F. Laine, *Fellow, IEEE*, Sarah H. Lisanby, and Angel V. Peterchev, *Member, IEEE*

***Abstract*—The goal of this study is to investigate the influence of white matter conductivity anisotropy on the electric field strength induced by electroconvulsive therapy (ECT). We created an anatomically-realistic finite element human head model incorporating tissue heterogeneity and white matter conductivity anisotropy using structural magnetic resonance imaging (MRI) and diffusion tensor MRI data. The electric field spatial distributions of three conventional ECT electrode placements (bilateral, bifrontal, and right unilateral) and an experimental electrode configuration, focal electrically administered seizure therapy (FEAST), were computed. A quantitative comparison of the electric field strength was subsequently performed in specific brain regions of interest thought to be associated with side effects of ECT (e.g., hippocampus and insula). The results show that neglecting white matter conductivity anisotropy yields a difference up to 19%, 25% and 34% in electric field strength in the whole brain, hippocampus, and insula, respectively. This study suggests that white matter conductivity anisotropy should be taken into account in ECT electric field models.**

I. Introduction

ELECTROCONVULSIVE therapy (ECT) is a therapeutic intervention in which electric currents are applied through scalp electrodes to induce a generalized seizure in anesthetized patients [1]. Although ECT plays a vital role in the treatment of medication-resistant psychiatric disorders, such as major depression, its use has been limited by its cognitive side effects (particularly amnesia) [2] and cardiac complications [3]. The therapeutic action and adverse side effects of ECT are dependent on the stimulus current parameters [4] and the electrode placement [5], but a complete mechanistic explanation for these relationships is lacking. For example, bifrontotemporal bilateral (BL) ECT causes higher cognitive side effects than right unilateral (RUL), putatively because BL ECT induces higher electric field strength in hippocampus and in other brain structures crucial for memory. Alternative ECT electrode configurations, such as bifrontal (BF) and focal electrically administered seizure therapy (FEAST), have been proposed with the goal of preferentially targeting prefrontal brain regions while avoiding stimulation in regions critical for amnestic side effects [6].

Previously, using an anatomically-realistic head model, we compared BL, RUL, BF, and FEAST ECT by quantifying the electric field in specific regions of interest (ROIs) with putative role in the therapeutic action and/or adverse side effects of ECT [7]. In that study we incorporated white matter anisotropic conductivity but did not quantify how this affected the electric field strength compared to an isotropic model. Indeed, recent investigations have indicated that the incorporation of tissue anisotropy in volume conductor models has a significant effect on the simulation results in EEG/MEG [8], [9], transcranial direct current stimulation [10]-[12], deep brain stimulation [13], and transcranial magnetic stimulation [14]. However, the effect of white matter conductivity anisotropy has not been quantified in ECT. In fact, other published models of the electric field or current density generated by ECT have not incorporated tissue conductivity anisotropy [15]-[17]. Since the electric field induced by ECT is typically widespread and reaches deep brain regions, and since depression itself is associated with regionally specific abnormalities in white matter fractional anisotropy [18], [19], it is reasonable to expect that the inclusion of anisotropic conductivity of the white matter would have a significant effect of the electric field distribution.

In this study, geometrically-accurate finite element models of the human head and the applied ECT electrodes are generated with or without incorporating white matter anisotropic conductivity derived from diffusion tensor MRI. The electric fields in the anisotropic and isotropic head models are quantitatively compared globally and in specific brain ROIs, e.g., the hippocampus and insula which may be associated with adverse side effects of ECT. This computational study allows us to examine the degree to which the white matter conductivity anisotropy affects the accuracy of the electric field solution. Enhanced accuracy of the ECT electric field models

Manuscript received April 15, 2011; revised June 20, 2011. This work was supported by NIH grant R01MH091083 and by the NSF through TeraGrid resources provided by NCSA under grant number TG-MCB100050.

W. H. Lee is with the Department of Biomedical Engineering, Columbia University, New York, NY 10027 and with the Department of Psychiatry and Behavioral Sciences, Duke University, Durham, NC 27710, USA (e-mail: wl2324@columbia.edu).

Z.-D. Deng is with the Department of Electrical Engineering, Columbia University, New York, NY 10027 and with the Department of Psychiatry and Behavioral Sciences, Duke University, Durham, NC 27710, USA (e-mail: zd2119@columbia.edu).

A. F. Laine is with the Department of Biomedical Engineering, Columbia University, New York, NY 10027, USA (e-mail: laine@columbia.edu).

S. H. Lisanby is with Department of Psychiatry and Behavioral Sciences, Duke University, Durham, NC 27710 and with the Division of Brain Stimulation and Therapeutic Modulation, Department of Psychiatry, Columbia University / New York State Psychiatric Institute, New York, NY 10032, USA (e-mail: sarah.lisanby@duke.edu).

A. V. Peterchev is with Departments of Psychiatry and Behavioral Sciences, Biomedical Engineering, and Electrical and Computer Engineering, Duke University, Durham, NC 27710, USA (phone: 919-684-0383; fax: 919-681-9962; e-mail: angel.peterchev@duke.edu).

could make them a better guide for interpretation of ECT studies and for improvements of ECT technique.

II. Methods

A. Finite Element Head Model

To construct the realistic head model, structural MR images were segmented into five different sub-regions including scalp, skull, cerebrospinal fluid, gray matter, and white matter. BrainSuite2 [20] was used to extract brain tissue compartments and cerebrospinal fluid regions including the ventricles. We then segmented the skull and scalp regions using the skull extraction algorithm based on a combination of thresholding and mathematical morphological operations including opening and closing [21].

For finite element mesh generation, we utilized the Computer Geometry Algorithm Library [22]. The mesh generator based on the labeled voxel-volume meshing technique allows generation of finite element tetrahedral meshes which contain one sub-mesh for each sub-domain and surface meshes which approximate the boundaries of the domain and sub-domains. This 3-D tessellation algorithm provides a discretized approximation of tissue compartments and their surface boundaries according to the restricted Delaunay tessellation paradigm [22]. The resulting finite element model of the head and the electrodes consists of approximately 1.6 million tetrahedral elements.

B. Electrical Conductivity Assignment

In the isotropic head model, the isotropic electrical conductivities were 9.8×10^5 S/m for the steel electrodes, 0.35 S/m for scalp, 0.0132 S/m for skull, 1.79 S/m for cerebrospinal fluid, 0.33 S/m for gray matter, 0.14 S/m for white matter [9]. In the anisotropic model, we estimated the white matter conductivity tensors under the assumption that the conductivity tenors share eigenvectors with the measured diffusion tensors [23]. The white matter anisotropic conductivity tensor was then modeled to be prolate rotationally-symmetric tensor ellipsoid with a fixed anisotropy ratio of 10:1 in each white matter voxel, yielding electrical conductivity estimates of 0.65 S/m and 0.065 S/m in the parallel (longitudinal) and perpendicular (transverse) to white matter fibers orientation, respectively [9].

C. ECT Electrode Configurations

We modeled three standard ECT electrode placements (BL, BF, and RUL) and an investigational configuration (FEAST [6], [24]) (see Fig. 1). Standard round electrodes (5 cm diameter) were modeled for the BL, BF, and RUL ECT configurations. For BL ECT, the two electrodes were centered bilaterally at the frontotemporal positions located 2.5 cm above the midpoint of the line connecting the external canthus and tragus. For BF ECT, the electrodes were placed bilaterally 5 cm above the outer angle of the orbit on a line parallel to the sagittal plane. For RUL ECT, one electrode was placed 2.5 cm to the right of vertex and the second electrode was in the right frontotemporal position. For FEAST, a larger rectangular electrode pad (2.5 cm × 6.3 cm) was placed over the right motor strip and a small circular electrode (2 cm diameter) over the right eyebrow.

D. ECT Simulation

The electric field distribution was computed with the finite element method software ANSYS (ANSYS Inc., Canonsburg, PA). For all electrode configurations, the current was set to 800 mA, corresponding to the conventional setting used with MECTA Spectrum 5000Q ECT devices (MECTA Corp., OR, USA). Since the frequencies used in ECT are relatively low (< 10 kHz), the electric field solution was obtained by solving the quasi-static Laplace equation with no internal sources [17], [25]

$$\nabla \cdot (\sigma \nabla \Phi) = 0 \tag{1}$$

where Φ and σ denote the electrical potential and the tissue electrical conductivity tensor, respectively. The Neumann boundary conductions apply on the head surface

$$(\sigma \nabla \Phi) \cdot \hat{n} = 0 \tag{2}$$

where $\hat{n}$ is the unit vector normal to the outer surface of the head. For each of the electrode configurations, the system of linear equations of the finite element method was solved using the preconditioned conjugate gradient solver. The gradient of the scalar potential Φ was then calculated to yield the electric field distribution inside the head.

E. Comparison of Electric Field Strength: Isotropy vs. Anisotropy

The electric field magnitudes were sampled in manually segmented ROIs thought to be relevant to adverse side effects

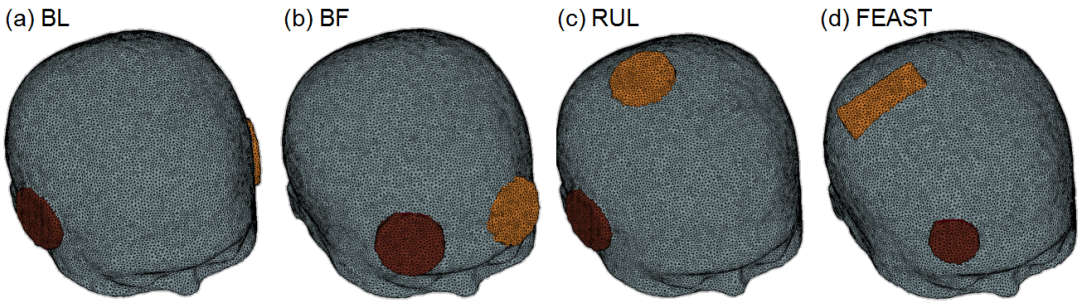

Fig. 1. 3-D finite element meshes for simulation of four ECT electrode configurations: (a) bilateral (BL), (b) bifrontal (BF), (c) right unilateral (RUL), and (d) focal electrically administered seizure therapy (FEAST). The models include six different compartments with distinct conductivities: five tissue layers (scalp, skull, cerebrospinal fluid, gray matter, and white matter) and the steel electrodes.

of ECT, including hippocampus and insula. We assessed the influence of white matter anisotropic conductivity on the induced electric field in these two regions and in the whole left and right hemispheres for the BL, BF, RUL, and FEAST electrode configurations. The difference between the electric field magnitude of the isotropic and anisotropic head models was quantified by a statistical measure of the relative error (RE) [10], defined as

$$\mathrm{RE} = \sqrt{\frac{\sum_{i=1}^{n} (E_i^{\mathrm{iso}} - E_i^{\mathrm{aniso}})^2}{\sum_{i=1}^{n} (E_i^{\mathrm{aniso}})^2}} \qquad (3)$$

where n is the number of samples in each of the ROIs, and E_i^{iso} and E_i^{aniso} denote the electric field magnitude of the isotropic and anisotropic head model, respectively.

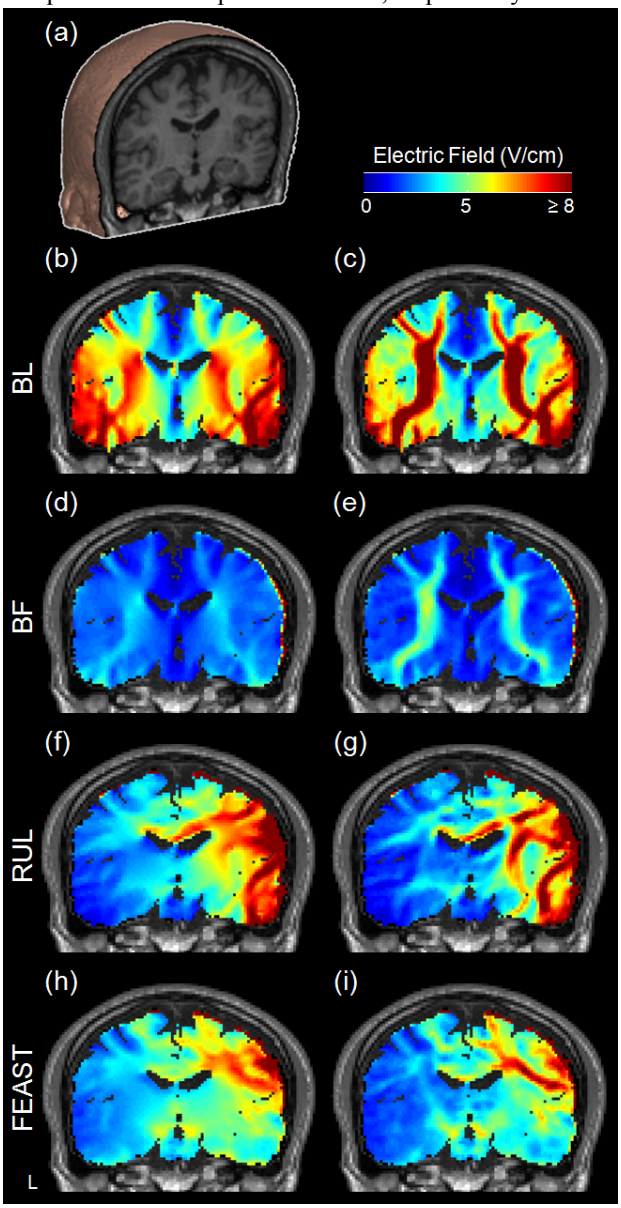

Fig. 2. (a) Cut-away 3-D rendering of the head model and the electric field magnitude spatial distribution in the isotropic (left column) and anisotropic (right column) head models for BL (b,c), BF (d,e), RUL (f,g), and FEAST (h,i) electrode configurations with 800 mA current. L: left.

TABLE I
PERCENTAGE RELATIVE ERROR BETWEEN ELECTRIC FIELD STRENGTH OF ISOTROPIC AND ANISOTROPIC MODELS FOR FOUR ECT ELECTRODE CONFIGURATIONS AND BRAIN ROIS ON LEFT (L) AND RIGHT (R) HEMISPHERES

ROI	BL		BF		RUL		FEAST	
	L	R	L	R	L	R	L	R
Whole hemisphere	19	18	10	6.3	16	6.6	14	5.6
Hippocampus	15	19	18	23	19	18	18	25
Insula	25	23	27	24	34	29	25	15

III. RESULTS

Fig. 1 shows the finite element model meshes for the BL, BF, RUL, and FEAST ECT electrode configurations. Fig. 2 shows the electric field magnitude distributions for the various ECT electrode configurations in a representative coronal slice of the isotropic (left column) and anisotropic (right) models. Compared to the isotropic models, in the anisotropic models current flow across the white matter fibers generates stronger electric field due to reduced electrical conductivity, and current flow along the white matter fibers generates weaker electric field due to increased conductivity.

Table I gives the results for RE in the left and right hemispheres and ROIs for the four ECT electrode configurations. Considering the whole brain, BL ECT produces the maximal error of 19% in the left hemisphere when white matter conductivity anisotropy is neglected. The minimal error of 6.3% corresponds to BF ECT in the right hemisphere. In the hippocampus, FEAST results in a maximal RE value of 25% in the right hemisphere, while the lowest error of 15% occurs with BL ECT in the left hemisphere. In the insula, RUL ECT results in the largest REs of 34% and 29% in the left and right hemispheres, respectively. The minimal error is 15% in the right hemisphere for the FEAST configuration.

IV. DISCUSSION AND CONCLUSIONS

A. Influence of White Matter Conductivity Anisotropy

We evaluated the influence of white matter conductivity anisotropy on the ECT electric field strength in the whole brain and in specific brain ROIs. Our results indicate that neglecting white matter conductivity anisotropy leads to a difference in the electric field strength up to 19% for the whole brain. In specific brain ROIs thought to be associated with side effects (hippocampus and insula), we found even higher differences—up to 34%. Errors of this size in ROIs with importance to the analysis of ECT paradigms motivate the inclusion of white matter conductivity anisotropy in computational electric field models.

Another important observation from Table I is that generally the error in the electric field strength between the isotropic and anisotropic models increases for brain regions that are farther away from the ECT electrodes. For example, although the overall RE in the brain is higher for BL than for BF, the RE in both hippocampus and insula is larger for BF than for BL. Notably, the BF electrodes are farther away from these brain regions compared to the BL electrodes. Similarly,

in the lateralized electrode configuration (RUL and FEAST), the electric field error in the left hemisphere and ROIs tends to be higher than on the right side (where the electrodes are placed). The sole exception is the RE in hippocampus for the FEAST configuration. The general trend for increasing error away from the electrodes could be explained in terms of the longer paths the electrical current has to traverse from the electrodes to distant brain regions, which results in a larger cumulative error of all the differences in conductivity along the current path. Thus, the incorporation of tissue anisotropy in the ECT electric field models is particularly important for analysis of the electric field characteristics in brain regions we try to avoid stimulating by placing the electrodes away from them. Typically these are brain regions thought to be associated with side effects, and thus the degree to which they are stimulated is of particular relevance to studies that evaluate ECT techniques aimed at improving safety. This observation further supports the inclusion of tissue anisotropic conductivity in ECT models.

B. Limitations

Future studies should consider several factors for refinement of the present model. In our anisotropic volume conductor model, we adopted the volume constraint algorithm to estimate the white matter anisotropic conductivity tensors with the assumption of a fixed anisotropy ratio of 10:1 in each white matter voxel [9]. However, this approach may overestimate the actual ratio of the white matter anisotropic conductivity tensors [8]. In reality, the ratio of the white matter anisotropic conductivity varies. In the present study, we did not examine alternative approaches for estimating the anisotropic tensors to account for this variability. Another limitation is the truncation of the head model at the level of the orbits, which affects the electric field strength and distribution [7]. However, this limitation is more relevant to the absolute electric field values, rather than the differential effects of anisotropic conductivity that are the focus of this paper. Nevertheless, to address this limitation, future models should be based on structural and diffusion tensor MRI data sets of the whole head.

V. References

[1] R. Abrams, *Electroconvulsive therapy*, 4th ed. New York: Oxford Unversity Press, 2002.

[2] H. A. Sackeim, J. Prudic, R. Fuller, J. Keilp, P. W. Lavori, and M. Olfson, "The cognitive effects of electroconvulsive therapy in community settings," *Neuropsychopharmacology,* vol. 32, pp. 244-254, 2007.

[3] G. A. Nuttall, M. R. Bowersox, S. B. Douglass, J. McDonald, L. J. Rasmussen, P. A. Decker, W. C. Oliver, and K. G. Rasmussen, "Morbidity and mortality in the use of electroconvulsive therapy," *J. ECT,* vol. 20, pp. 237-241, 2004.

[4] A. V. Peterchev, M. A. Rosa, Z. D. Deng, J. Prudic, and S. H. Lisanby, "Electroconvulsive therapy stimulus parameters: rethinking dosage," *J. ECT,* vol. 26, pp. 159-174, 2010.

[5] C. H. Kellner, K. G. Tobias, and J. Wiegand, "Electrode placement in electroconvulsive therapy (ECT): A review of the literature," *J. ECT,* vol. 26, pp. 175-180, 2010.

[6] H. A. Sackeim, "Convulsant and anticonvulsant properties of electroconvulsive therapy: towards a focal form of brain stimulation," *Clin. Neurosci. Res.,* vol. 4, pp. 39-57, 2004.

[7] W. H. Lee, Z. D. Deng, T. S. Kim, A. F. Laine, S. H. Lisanby, and A. V. Peterchev, "Regional electric field induced by electroconvulsive therapy: A finite element simulation study," *Conf. Proc. IEEE Eng. Med. Biol. Soc.*, pp. 2045-2048, 2010.

[8] D. Gullmar, J. Haueisen, and J. R. Reichenbach, "Influence of anisotropic electrical conductivity in white matter tissue on the EEG/MEG forward and inverse solution. A high-resolution whole head simulation study," *NeuroImage,* vol. 51, pp. 145-163, 2010.

[9] C. H. Wolters, A. Anwander, X. Tricoche, D. Weinstein, M. A. Koch, and R. S. MacLeod, "Influence of tissue conductivity anisotropy on EEG/MEG field and return current computation in a realistic head model: A simulation and visualization study using high-resolution finite element modeling," *NeuroImage,* vol. 30, pp. 813-826, 2006.

[10] W. H. Lee, H. S. Seo, S. H. Kim, M. H. Cho, S. Y. Lee, and T. S. Kim, "Influence of white matter anisotropy on the effects of transcranial direct current stimulation: a finite element study," *Int. Conf. Biomed. Eng.,* pp. 460-464, 2009.

[11] T. F. Oostendorp, Y. A. Hengeveld, C. H. Wolters, J. Stinstra, G. van Elswijk, and D. F. Stegeman, "Modeling transcranial DC stimulation," *Conf. Proc. IEEE Eng. Med. Biol. Soc.,* pp. 4226-4229, 2008.

[12] H. S. Suh, W. H. Lee, Y. S. Cho, J. H. Kim, and T. S. Kim, "Reduced spatial focality of electrical field in tDCS with ring electrodes due to tissue anisotropy," *Conf. Proc. IEEE Eng. Med. Biol. Soc.,* pp. 2053-2056, 2010.

[13] C. R. Butson, S. E. Cooper, J. M. Henderson, and C. C. McIntyre, "Patient-specific analysis of the volume of tissue activated during deep brain stimulation," *NeuroImage,* vol. 34, pp. 661-670, 2007.

[14] M. De Lucia, G. J. M. Parker, K. Embleton, J. M. Newton, and V. Walsh, "Diffusion tensor MRI-based estimation of the influence of brain tissue anisotropy on the effects of transcranial magnetic stimulation," *NeuroImage,* vol. 36, pp. 1159-1170, 2007.

[15] M. Nadeem, T. Thorlin, O. P. Gandhi, and M. Persson, "Computation of electric and magnetic stimulation in human head using the 3-D impedance method," *IEEE Trans. Biomed. Eng.,* vol. 50, pp. 900-907, 2003.

[16] M. Sekino and S. Ueno, "Comparison of current distributions in electroconvulsive therapy and transcranial magnetic stimulation," *J. Appl. Phys.,* vol. 91, pp. 8730-8732, 2002.

[17] M. Sekino and S. Ueno, "FEM-based determination of optimum current distribution in transcranial magnetic stimulation as an alternative to electroconvulsive therapy," *IEEE Trans. Magn.,* vol. 40, pp. 2167-2169, 2004.

[18] M. S. Korgaonkar, S. M. Grieve, S. H. Koslow, J. D. Gabrieli, E. Gordon, and L. M. Williams, "Loss of white matter integrity in major depressive disorder: Evidence using tract-based spatial statistical analysis of diffusion tensor imaging," *Hum. Brain Mapp.,* 2010.

[19] F. Wu, Y. Tang, K. Xu, L. Kong, W. Sun, F. Wang, D. Kong, Y. Li, and Y. Liu, "Whiter matter abnormalities in medication-naive subjects with a single short-duration episode of major depressive disorder," *Psychiatry Res.,* vol. 191, pp. 80-83, 2011.

[20] D. W. Shattuck and R. M. Leahy, "BrainSuite: An automated cortical surface identification tool," *Med. Image Anal.,* vol. 6, pp. 129-142, 2002.

[21] B. Dogdas, D. W. Shattuck, and R. M. Leahy, "Segmentation of skull and scalp in 3-D human MRI using mathematical morphology," *Hum. Brain Mapp.,* vol. 26, pp. 273-285, 2005.

[22] CGAL, Computational Geometry Algorithms Library [Online]. Available: http://www.cgal.org

[23] P. J. Basser, J. Mattiello, and D. LeBihan, "MR diffusion tensor spectroscopy and imaging," *Biophys. J.,* vol. 66, pp. 259-267, 1994.

[24] T. Spellman, A. V. Peterchev, and S. H. Lisanby, "Focal electrically administered seizure therapy: a novel form of ECT illustrates the roles of current directionality, polarity, and electrode configuration in seizure induction," *Neuropsychopharmacology,* vol. 34, pp. 2002-2010, 2009.

[25] C. A. Bossetti, M. J. Birdno, and W. M. Grill, "Analysis of the quasi-static approximation for calculating potentials generated by neural stimulation," *J. Neural Eng.,* vol. 5, pp. 44-53, 2008.